DEVELOPMENT OF FAILURE CRITERION FOR MATERIALS EXPOSED TO MULTIAXIAL TENSILE-TORSION TESTING

By

DAVID WILLIAM MILLAR

AN HONORS THESIS PRESENTED TO THE
COLLEGE OF MECHANICAL AND AEROSPACE ENGINEERING
AT THE UNIVERSITY OF FLORIDA IN PARTIAL FULFILLMENT
OF THE REQUIREMENTS FOR THE DEGREE OF
BACHELOR OF SCIENCE WITH HIGH HONORS

UNIVERSITY OF FLORIDA

2018

To Maya for staying by my side and believing in me, no matter what.

ACKNOWLEDGEMENTS

I want to express my gratitude to Dr. Peter G. Ifju and Mattlock Mennu for supervising my research work. Dr. Ifju sparked my interest in Mechanics and Materials and has always encouraged me to get involved and learn more about the field through positions under his various Master's and Ph.D. students. Without his encouragement and motivation for me to succeed, this project may not have happened or gotten as far as it did. I am grateful for all his help and look forward to working with him further on this project as I continue my studies as a Master's student at the University of Florida. And without the helpful assistance of Mattlock, the testing portion of this project could not have happened. Lastly, I want to thank my family and friends at UF for their support and constant encouragement throughout this process.

TABLE OF CONTENTS

LIST OF TABLES

LIST OF FIGURES

LIST OF ABBREVIATIONS & SYMBOLS

Abbreviations

UTM = Universal Testing Machine

ABS = Acrylonitrile, Butadiene, and Styrene

EDM = Electrical Discharge Machining

DAQ = Data Acquisition

Symbols

σ = Normal tensile stress

ε = Normal strain

τ = Shear stress

Y = Yield (as in stress)

U = Ultimate (as in stress)

P = Load

T = Torque

M = Moment

ϕ = Degree of Twist

J = Polar Moment of Inertia

C = radius of test specimen

Abstract of Thesis Presented to the
College of Mechanical and Aerospace Engineering at the
University of Florida in Partial Fulfillment of the Requirements
of Graduating with High Honors

DEVELOPMENT OF FAILURE CRITERION FOR MATERIALS EXPOSED TO MULTIAXIAL TENSILE-TORSION TESTING

By

David William Millar

April 2018

Chair: Dr. Peter Ifju
Major: Mechanical Engineering

Multiaxial fatigue tests permit advances in the basic understanding of materials behavior that might be utilized in the processes of declaring component service lives. To accurately predict how a material will behave when exposed to multiple sources of stress, we set out with the intent to develop testing methods that can be applied to the testing of brittle and ductile materials in one comprehensive failure test that will yield accurate failure criterion for combined tensile stress and torsional forces. To do this we studied the current failure criterion methods of a specific material (ABS plastic) to accurately describe and predict behavior of this material in between areas of pure shear and pure tension, i.e. multiaxial failure. Individual tensile and torsion tests were run to establish a baseline for the material's failure criterion, then multiaxial tests were run and compared to the established criterion. The behavior observed and the placement of the mixed tensile and torsional stress on the material's established failure graph allowed us to see that the test method worked, and accurate results were achieved.

SECTION I
INTRODUCTION & MOTIVATION

Uniaxial testing methods, such as pure tensile, pure compression, or pure torsion tests, are the most common way to determine a material's mechanical properties. However, when being implemented into real-world applications, materials are often exposed to more than just uniaxial forces. Because of this, multiaxial fatigue tests permit advances in the basic understanding of materials behavior that might be utilized in the processes of declaring component service lives [1]. Similar to uniaxial testing methods, multiaxial testing applies loading to a single specimen, but uses several actuators to directly apply a multiaxial load [2].

Multiaxial Tension/Torsion Testing

One of the most common multiaxial tests involves tensile-torsion testing, or combined axial and torsional loading [3]. Common to composites testing applications, tension-torsion testing can replicate anticipated or recorded service loading conditions that involve combinations of axial or linear loading with torsional or rotary loading [3]. When a specimen is loaded into a uniaxial testing machine, it is subjected to uniaxial stress or strain; essentially, the specimen is either being pulled or pushed in one direction (the 11 direction), while all other components (i.e. 12, 21, 32, etc.) of stress and strain are zero [4]. For an isotropic material, the stress and stain experienced can be characterized by the following matrices:

$$[\sigma] = \begin{bmatrix} \sigma_A & 0 & 0 \\ 0 & \sigma_L & 0 \\ 0 & 0 & \sigma_L \end{bmatrix}; [\varepsilon] = \begin{bmatrix} \varepsilon_A & 0 & 0 \\ 0 & \varepsilon_L & 0 \\ 0 & 0 & \varepsilon_L \end{bmatrix} \tag{1}$$

In (1), the subscript "A" stands for axial, while "L" stands for lateral. Thus, for uniaxial stress, (1) can simply be written as:

$$[\sigma] = \begin{bmatrix} \sigma_A & 0 & 0 \\ 0 & 0 & 0 \\ 0 & 0 & 0 \end{bmatrix}; [\varepsilon] = \begin{bmatrix} \varepsilon_A & 0 & 0 \\ 0 & 0 & 0 \\ 0 & 0 & 0 \end{bmatrix} \tag{2}$$

While (1) and (2) are useful in determining stress and stain of a material in a single direction, they fail to account for stresses experienced in the auxiliary directions. Therefore, multiaxial tests are useful in that they can characterize behavior over a wide range of loading ratios and conditions [3].

For example, high force/torque machines, such as the TestResources 300 Series Universal Testing Machine (UTM), can be used to generate constitutive modeling of tubular test specimens [3]. These types of machines can generate large plastic strains on test specimens without complications to the stress state that occur when necking begins to take place [5]. During these combination tests, the state of stress in the torsion test consists of pure shear, with equal tensile and compressive stresses at 45º to the shear stresses; a variation in the stress state can be achieved if axial forces, tensile or compressive, are superimposed on the twisting moment [5].

However, like most testing methods, multiaxial testing is not without it's flaws. The chief disadvantage of the torsion component of the test is that stress, strain, and strain rate can significantly vary from the axis to the outer fiber of a solid cylindrical specimen [5]. Despite this, accurate measurements and characteristics can still be determined by using hollow cylindrical specimen with a relatively thin wall thickness [5].

Development of Failure Criterion – Ductile Materials

As stated previously, multiaxial testing methods can be used to quantify component service life. Another way service life can be maximized is by studying the failure (yield) criterion of the test material, or the relationship among the stresses which predict the yielding of the material [6]. There are two yield criteria that are commonly used by engineers in industry: Tresca criterion - also called maximum shear stress theory, and von Mises yield criterion – also called distortion

energy criterion [6]. Each of these studies when plastic deformation will occur in materials to develop material specific yield criteria.

The Tresca criterion focuses on shear stress in a material. According to Beer et. al., Tresca criterion is based on the observation that yield in ductile materials is caused by slipping of material along surfaces and caused by shearing stresses [7]. Tresca criterion further states that a specimen will not fail if the maximum shear stress (i.e. τ_{max}) remains smaller than the corresponding shear stress in a tensile-test specimen of the same material as the specimen starts to yield [7]. In other words,

$$\tau_{max} = \tau_Y$$
$$\text{where } \tau_{max} = \frac{\sigma_a - \sigma_b}{2} = \frac{\sigma_Y}{2} \tag{3}$$

In (3), σ_a and σ_b are the principal stresses. If the principal stresses have the same sign, the Tresca criterion gives (4); if the principal stresses have opposite signs, Tresca criterion gives (5).

$$|\sigma_a| < \sigma_Y \quad |\sigma_b| < \sigma_Y \tag{4}$$

$$|\sigma_a - \sigma_b| < \sigma_Y \tag{5}$$

The von Mises criterion focuses on normal stress in a material. According to Beer et. al., von Mises criterion is based on the determination of the distortion energy in a material [7]. According to this criterion, a specimen will not fail if the maximum value of the distortion energy per unit volume in that material remains smaller than the distortion energy per unit volume required to cause yield in a tensile-test specimen of the same material [7]. In other words,

$$\sigma_a^2 - \sigma_a\sigma_b + \sigma_b^2 < \sigma_Y^2 \tag{6}$$

In (6), σ_a and σ_b are the principal stresses. When a specimen starts to yield, von Mises gives (7); the limit of the von Mises yield criterion is given by (8).

$$\sigma_a = \sigma_Y \qquad \sigma_b = 0 \tag{7}$$

$$\sigma_a^2 - \sigma_a\sigma_b + \sigma_b^2 = \sigma_Y^2 \tag{8}$$

To better understand failure criterion, values from both the Tresca and von Mises criterion can be plotted along axes of principal stresses, as seen in Fig. 1 and Fig. 2. Any given state of stress can be represented by a point of coordinates σ_a and σ_b. If a stress point falls within the boundary lines of either stress criterion, the specimen will not fail; conversely, if the point falls outside the boundary lines of either stress criterion, the specimen will fail as a result of yield in the material [7].

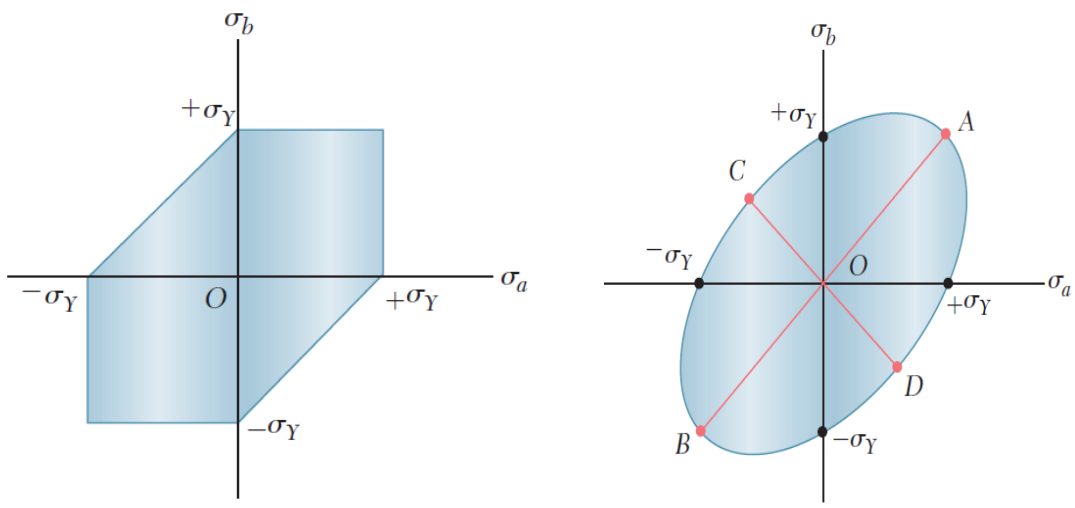

Fig. 1. Tresca's hexagon for the maximum-shearing-stress criterion (left); von Mises surface based on the maximum-distortion-energy criterion (right) [7].

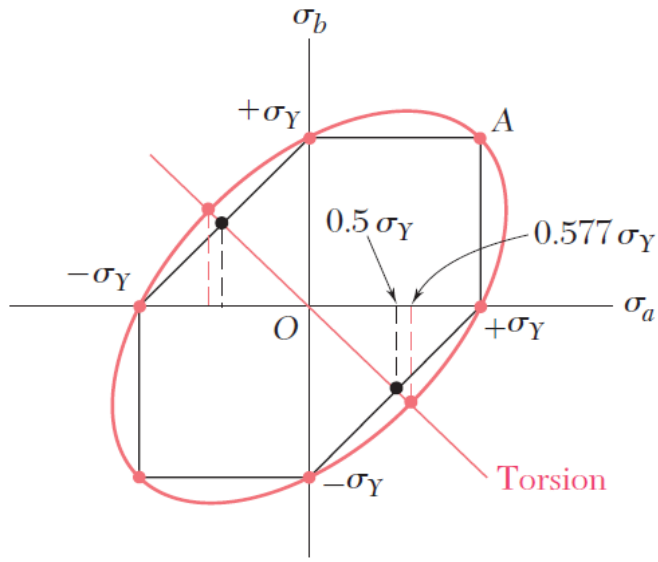

Fig. 2. Comparison of the Tresca hexagon and von Mises surface for failure criterion [7].

Development of Failure Criterion – Brittle Materials

While Tresca and von Mises can establish failure criterion for most materials, there are additional failure criterion for brittle materials. When subjected uniaxial testing, brittle materials – such as Acrylonitrile, Butadiene, and Styrene (ABS) plastic – rupture (or fracture) with little to no plastic deformation before failure [7]. When a brittle specimen is under uniaxial stress, the normal stress causing failure is equal to the ultimate tensile strength (σ_U) [7].

One main failure criterion for brittle materials is Coulomb's criterion, also known as the maximum-normal-stress criterion [7]. Coulomb's criterion states a specimen will fail when the maximum normal stress reaches the ultimate strength (σ_U) obtained from the tensile test of a specimen of the same material [7]. In other words, the material will not fail as long as:

$$|\sigma_a| < \sigma_U \quad |\sigma_b| < \sigma_U \tag{9}$$

Similar to Tresca and von Mises, Coulomb's criterion can be better understood graphically, as seen in Fig. 3. If a stress point falls within the boundary lines, the specimen will not fail; conversely, if the point falls outside the boundary lines, the specimen will fail [7].

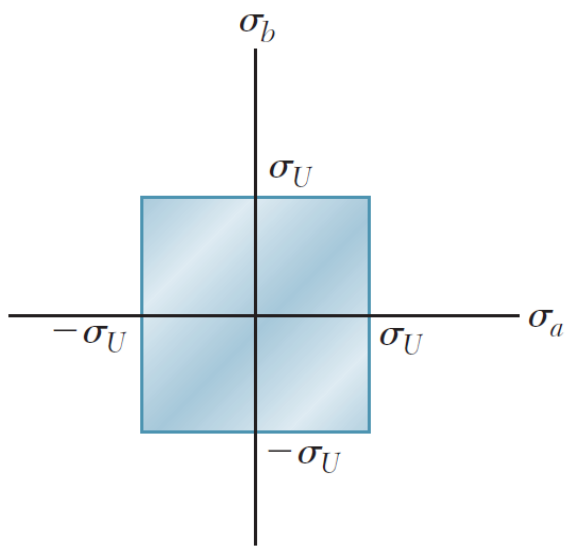

Fig. 3. Coulomb's surface for the maximum-normal-stress criterion [7].

Focus on Testing – Prevent Slipping with EDM

Another disadvantage with multiaxial tensile-torsion testing is slipping of the test specimen during testing. Slipping can cause inaccurate data to be collected and, therefore, inaccurate failure criterion can be established. To better accommodate such testing, specialized grips can be manufactured to better grab the specimen and prevent slippage. One such way the grips can be modified is through the use of electrical discharge machining (EDM).

EDM has been in use in industry for about 50 years [8]. In standard EDM, an electrical spark is created between an electrode and the part to be machined, usually a steel/metallic alloy. The spark is carefully controlled and localized and can reach intense heat, with temperatures reaching 8,000 – 12,000°C [9]. To control the process, the workpiece is typically placed in the dielectric (electrical insulator) of deionized water; the water acts as a conductor and a good coolant to flush away the eroded metal particles [9]. When special contours need to be cut that a spark won't be able to cut accurately, wire EDM is used. In wire EDM, a metallic wire is placed between

the conductors and the electrical current is run through it; the wire is then used to cut a programmed contour in a workpiece, typically using CNC machines [8-9].

Motivation

When attempting to establish failure criterion for a material, the type of test and material being used must be considered. Often, ductile materials will require different testing methods than brittle materials due to their unique behaviors when exposed to stress. Additionally, to gain a more comprehensive idea of failure criterion, multiple tests of different failure modes, such as tensile and torsional stress, will need to be tested. Because of this, failure testing of materials, in either research or industry, is often cost prohibited, in terms of both time and money.

The degree of ineffectiveness of multiple failure tests of a single material is usually determined from how often a failure test needs to be conducted for a single material. Attempts to remedy this can still be considered ineffective due to the extra cost associated with specialized multiaxial testing equipment. Therefore, we intend to develop testing methods that can be applied to the testing of brittle and ductile materials in one comprehensive failure test that will yield accurate failure criterion for combined tensile stress and torsional forces. To do so, we first intend to study current failure criterion methods of a specific material (ABS plastic) to accurately describe and predict behavior of this material in between areas of pure shear and pure tension, i.e. multiaxial failure. Once we have established accurate proof of accurate testing and failure criterion, the goal will be to test with a variety of new materials before establishing and verifying the new testing method.

SECTION II
PROCEDURES

Pre-Experimentation

Before multiaxial testing could commence, possible causes of error in the testing procedure needed to be eliminated, starting with the test specimen and chuck grips. The original chuck grips for the TestResources 300 Series UTM, as seen in Fig. A-1, have a very small contact area, meaning that slipping is likely to occur during any of the tests. To minimize the risk of slipping, the contact area needed to be expanded on both the specimen and grips so the resultant force and moment generated mimic the behavior of a wrench when tightening a bolt, as seen in Fig. 4.

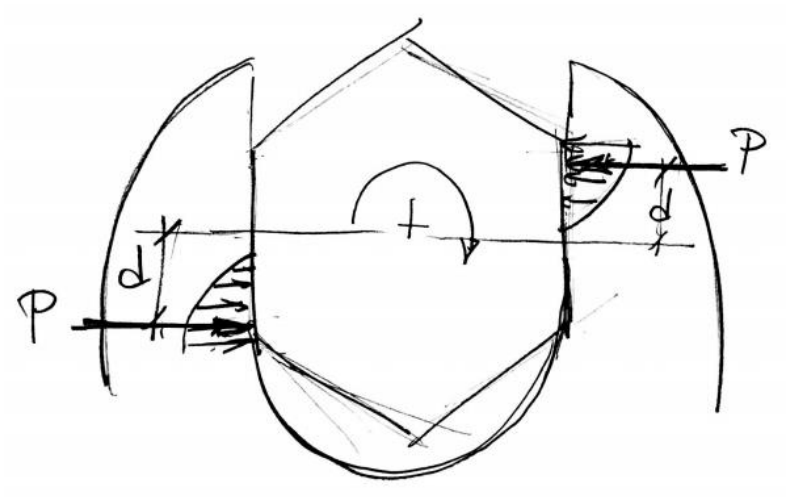

Fig. 4. Behavior of a wrench twisting a bolt. The resultant forces on either face of the bolt-head help in generate a moment on the bolt and assist in twisting.

To accomplish this, models of the specimen and chuck grips were generated in Solidworks. The specimens were designed to be hexagonal dogbone in shape; additionally, three of the specimen's faces contain semi-circular inclusions, as seen in Fig. A-3. The chuck grips were modified to contain an extruded semi-circular slot that would fit into three of the specimen's faces, as seen in Fig. A-2. Once the designs for each were finalized, the chuck grips were shipped to

Triad EDM, a local manufacturing company that specializes in wire EDM. Wire EDM was used to cut the face of grips down to match the designed faces in Fig. A-2.

While the grips were being machined, the specimens needed to be manufactured; therefore, a test material needed to be chosen. To accommodate for the timeline of the project, but still provide significant results to establish "proof-of-concept," the specimens were printed in the UF MAE 3D Printing Lab using ABS plastic. Relevant material properties for ABS plastic are given by Table I.

TABLE I
Mechanical Properties of ABS Plastic

Property	Symbol	Value
Density	ρ	3.79E-02 lb./in^3
Rockwell A Hardness	HRA	102
Ultimate Tensile Strength	σ_U	5.54 ksi
Yield Tensile Strength	σ_Y	5.99 ksi
Young's Modulus	E	305 ksi
Flexural Yield Strength	σ_{bend}	9.28 ksi
Flexural Modulus	E_{bend}	319 ksi

*All values in Table I were found using [10].

Experimentation & Analysis

With the specimens printed and the grips modified, testing commenced. The newly modified grips were loaded into the UTM's chucks and attached to the machine's multiaxial actuators. As seen in Fig. 5, the specimen was loaded into the chuck, where the three grips were screwed in until the new extrusions were fully inserted into the specimen's slots. As seen in Fig. 6, the test specimens were tested under three different loading conditions: {1} pure tension, {2} pure torsion, and {3} multiaxial tension and torsion. For test {1}, appropriate testing rates in inches/second were applied; for test {2}, appropriate testing rates in degrees/second were applied.

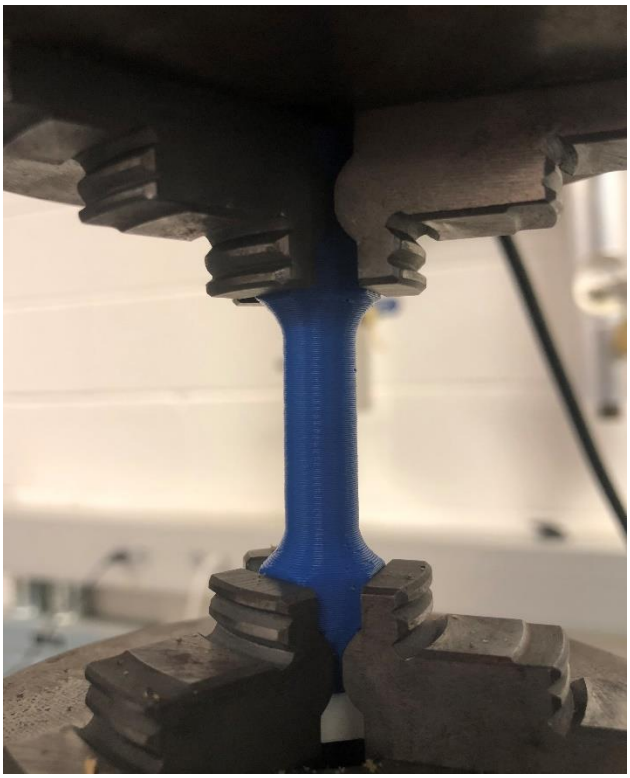

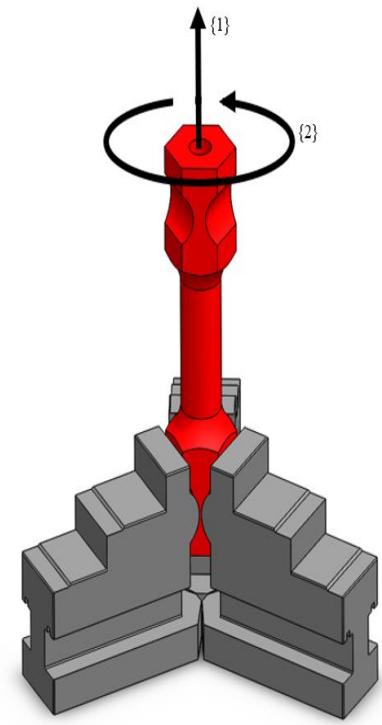

Fig. 5. Physical test specimen loaded into the UTM's grips (right); Fig. 6. Model of specimen loaded into grips (only bottom grips shown), with testing conditions indicated. Test {3} is a combination of {1} and {2} shown above (left).

After each test, the data recorded by the SADI data acquisition (DAQ) device was exported to an Excel spreadsheet; on each spreadsheet, appropriate data for each test was analyzed to generate stress vs. strain or torque vs. degree-of-twist curves.

For test {3}, material data from the curves generated from tests {1} and {2} were used to generate updated testing rates for the two tests being run simultaneously. Equations (10) and (11) were used to determine the updated testing rates to ensure that failure for the pure tension and pure torsion tests would occur at or around 120 seconds.

$$\text{Updated tension testing rate} = P_{rate,new} = \frac{Failure\ Deflection\ (in)}{Desired\ Failure\ Time\ (s)} \tag{10}$$

$$\text{Updated torsion testing rate} = T_{rate,new} = \frac{Failure\ Twist\ Angle\ (deg)}{Desired\ Failure\ Time\ (s)} \tag{11}$$

After several trials of test {3}, the data recorded by the SADI DAQ was exported to an Excel spreadsheet; on these spreadsheets, the ratio of tensile load (P) to torsional torque (T) was plotted against deflection. This data, along with the previous curves from tests {1} and {2}, was then used to determine if the failure behavior witnessed accurately described theoretical behavior of this material in between areas of pure shear and pure tension.

SECTION III
EXPERIMENTATION AND RESULTS

In Fig. 7 through Fig. 9, the data from the pure tension test of the ABS plastic specimen was analyzed to yield appropriate stress vs. strain curves. The data that resulted exhibited properties of a brittle material, as expected. This can be seen by the fact that the graph reaches the failure point without entering a plastic deformation region. This behavior can also be seen in the failure mode exhibited by the physical specimen in Fig. B-1.

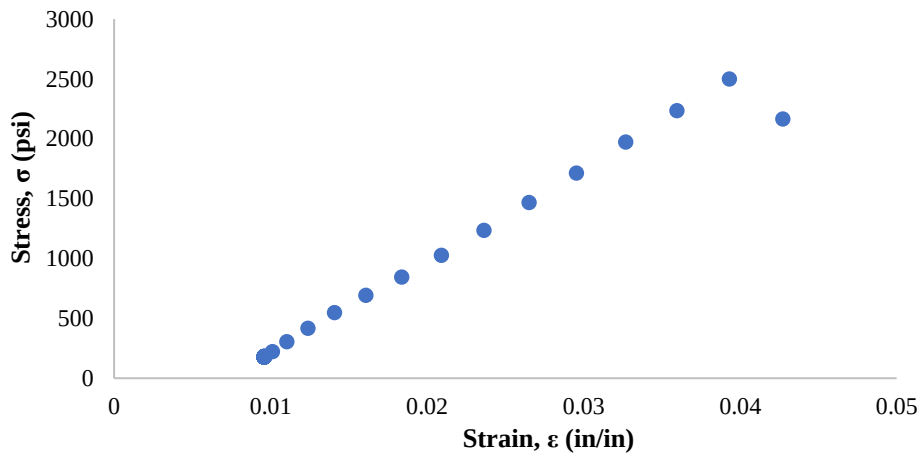

Fig. 7. Strain (in/in) vs. Stress (psi) curve for the pure tension test of the ABS test specimen at a testing speed of 7.00 inches/second.

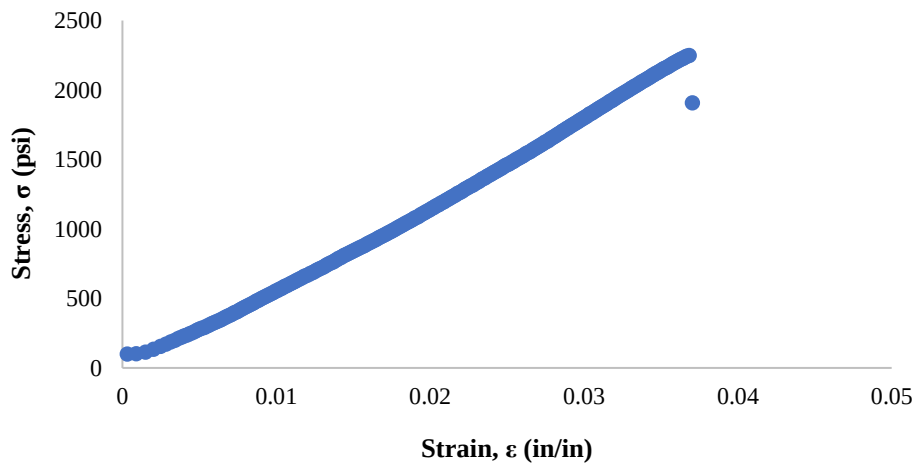

Fig. 8. Strain (in/in) vs. Stress (psi) curve for the pure tension test of the ABS test specimen at a testing speed of 0.05 inches/second.

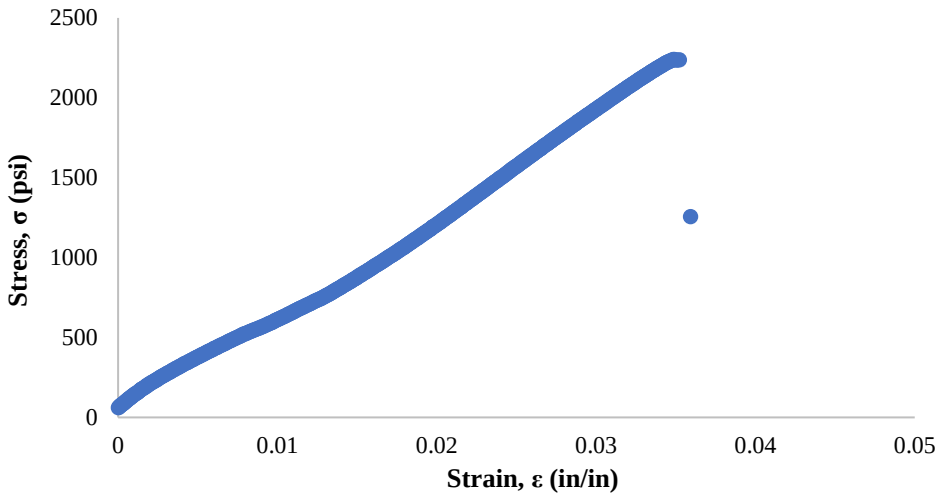

Fig. 9. Strain (in/in) vs. Stress (psi) curve for the pure tension test of the ABS test specimen at a testing speed of 0.025 inches/second.

In Fig. 10 and Fig. 11, the degree of twist and torque data from the pure torsion tests of the ABS plastic specimen are plotted against each other. The data that resulted from subjecting the specimen to a pure torsion force exhibited properties of a brittle material, as expected. This can be seen by the fact that the graph reaches the failure point without entering a plastic deformation region. This behavior can also be seen in the failure mode exhibited by the physical specimen in Fig. B-2.

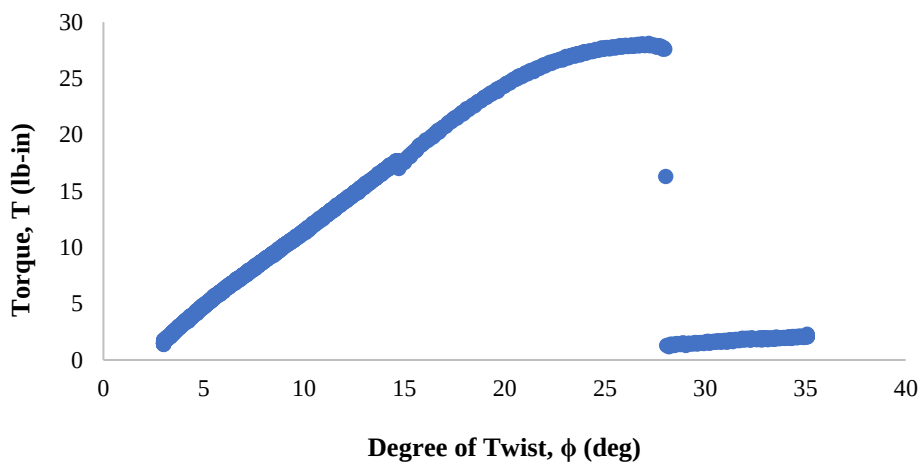

Fig. 10. Degree of Twist (deg) vs. Torque (lb.-in) curve for the pure tension test of the ABS test specimen at a testing speed of 0.25 degrees/second.

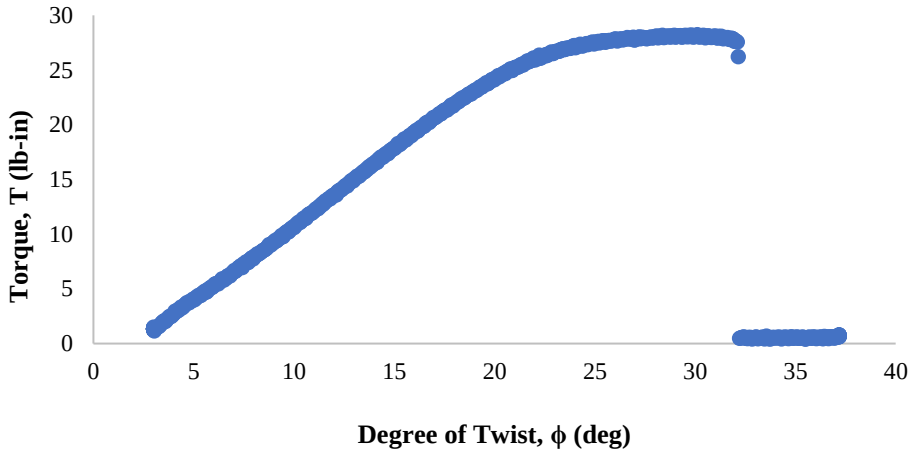

Fig. 11. Degree of Twist (deg) vs. Torque (lb.-in) curve for the pure tension test of the ABS test specimen at a testing speed of 0.50 degrees/second.

In Fig.12 through Fig. 20, the stress/strain, torque/twist, and combined data are plotted. All three multiaxial failure trials were run at simultaneous rates of 0.000293 inches/second and 0.1495 degrees/second, as calculated using (10) and (11). The material failed with two distinct failure modes; the first was flat, which is typical of brittle materials when exposed to pure tension (see Fig. B-1), and the second was perpendicular (about 45º) to the shaft axis (see Fig. B-2). This combined behavior can be seen in the failure mode exhibited by the physical specimen in Fig. B-3 through Fig. B-4.

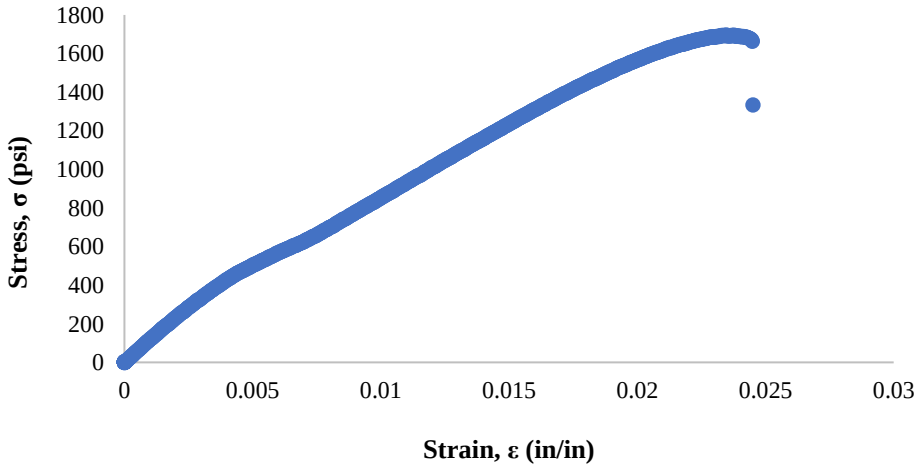

Fig. 12. Strain (in/in) vs. Stress (psi) curve for the multiaxial tension-torsion test of the first (blue) ABS test specimen.

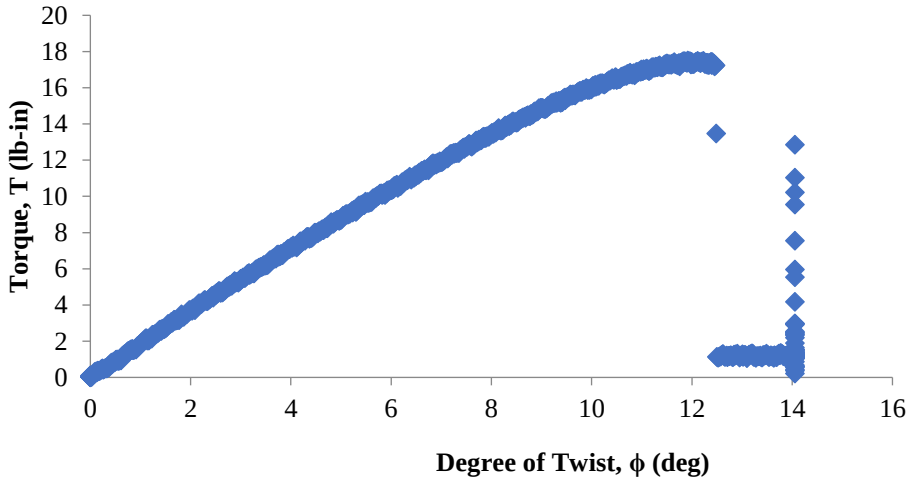

Fig. 13. Degree of Twist (deg) vs. Torque (lb.-in) curve for the multiaxial tension-torsion test of the first (blue) ABS test specimen.

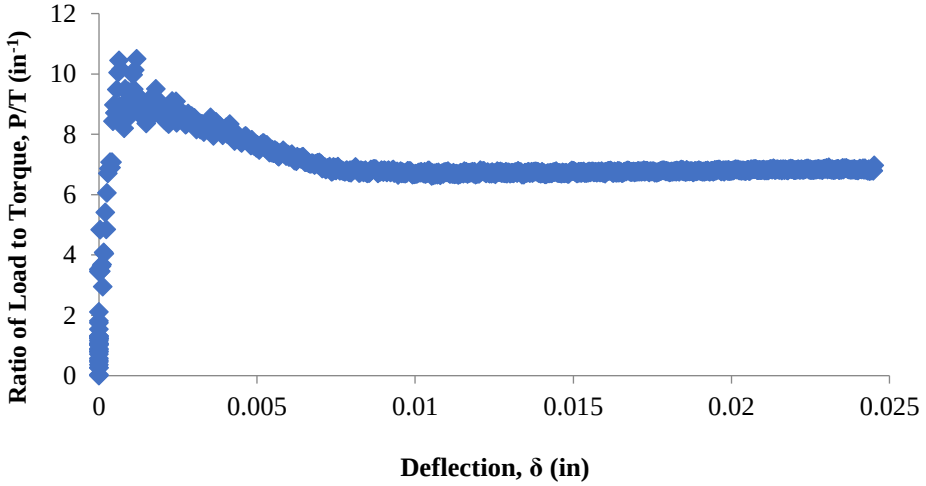

Fig. 14. Deflection (in) vs. Ratio of Load to Torque (in^{-1}) curve for the multiaxial tension-torsion test of the first (blue) ABS test specimen.

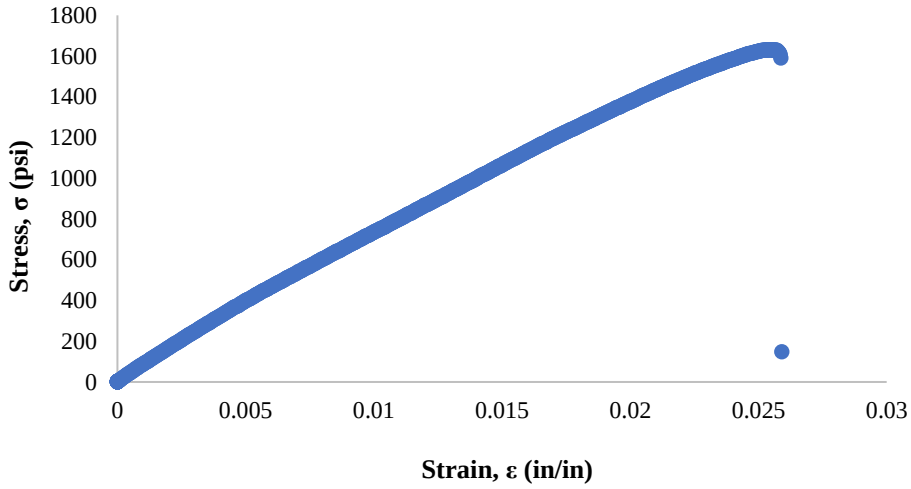

Fig. 15. Strain (in/in) vs. Stress (psi) curve for the multiaxial tension-torsion test of the second (grey) ABS test specimen.

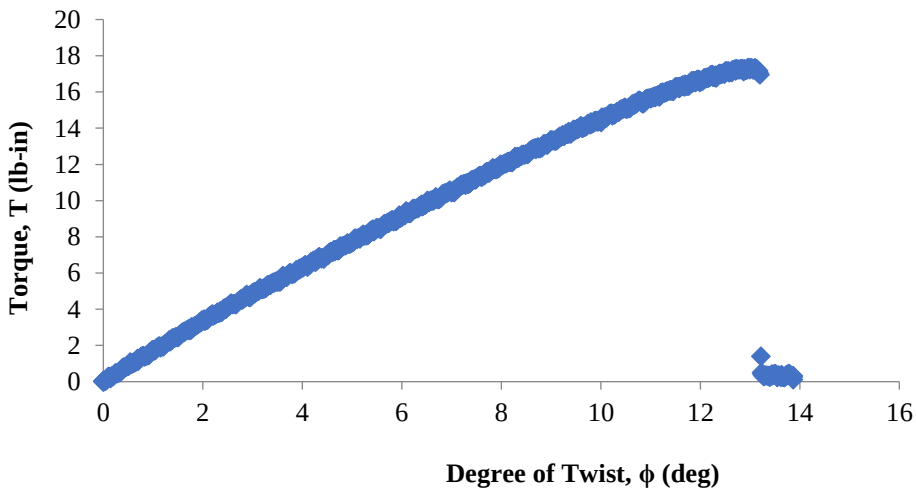

Fig. 16. Degree of Twist (deg) vs. Torque (lb.-in) curve for the multiaxial tension-torsion test of the second (grey) ABS test specimen.

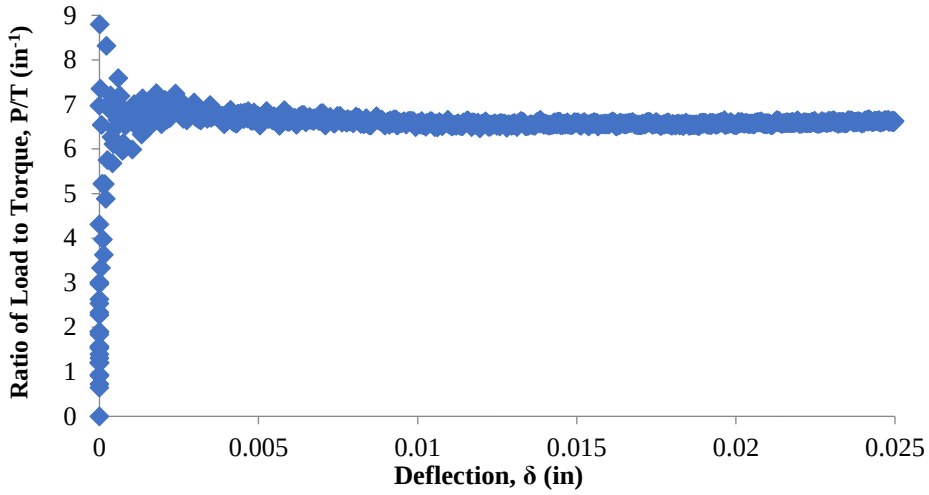

Fig. 17. Deflection (in) vs. Ratio of Load to Torque (in^{-1}) curve for the multiaxial tension-torsion test of the second (grey) ABS test specimen.

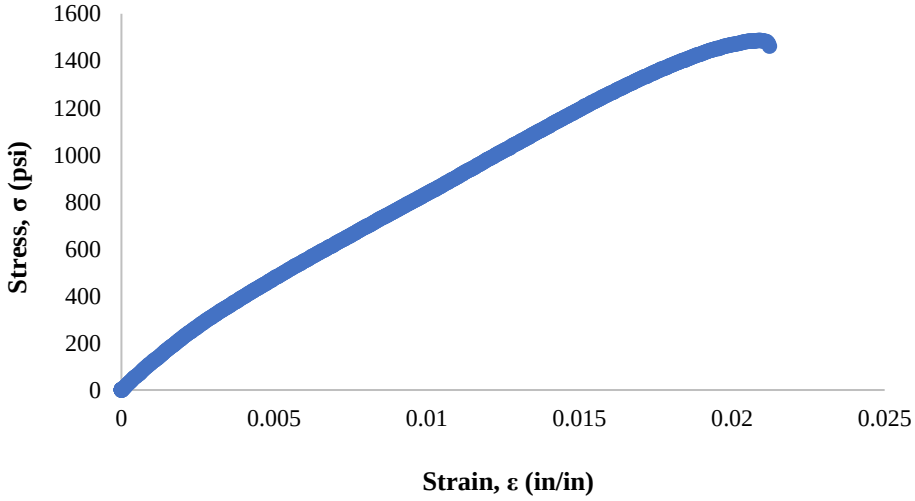

Fig. 18. Strain (in/in) vs. Stress (psi) curve for the multiaxial tension-torsion test of the third (red) ABS test specimen.

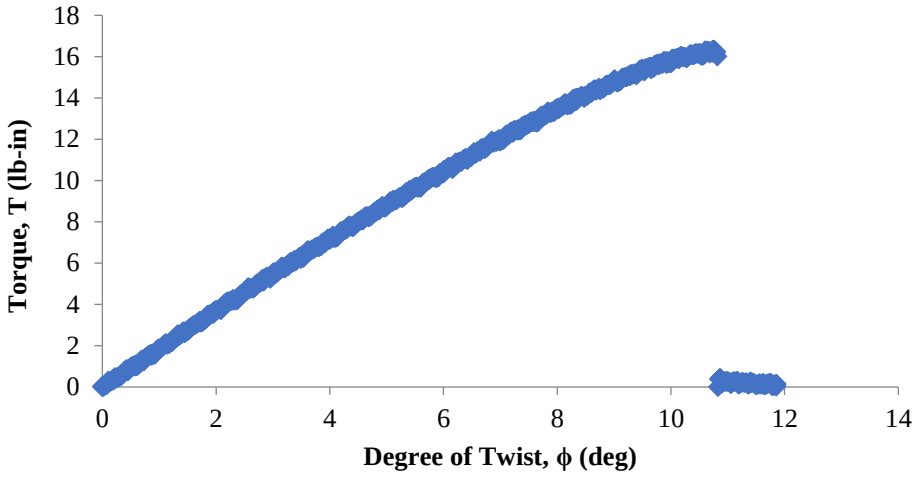

Fig. 19. Degree of Twist (deg) vs. Torque (lb.-in) curve for the multiaxial tension-torsion test of the third (red) ABS test specimen.

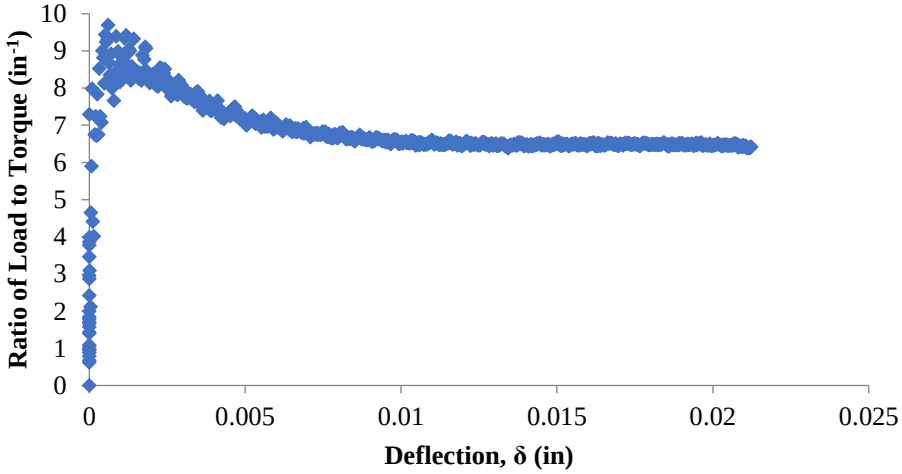

Fig. 20. Deflection (in) vs. Ratio of Load to Torque (in^{-1}) for the multiaxial tension-torsion test of the third (red) ABS test specimen.

SECTION IV
DISCUSSION OF EXPERIMENTATION AND RESULTS

During the testing of pure tension, the first test was run at an initial speed of 7.00 inches per second. This yielded in the robust curve as seen in Fig. 7. Therefore, for the remaining tests run for pure tension, the testing rate was reduced to 0.05 and 0.025 inches per second, so the data would be more precise and yield consistent data. This same approach was also applied to the pure torsion tests; here the testing rates started small -at 0.25 degrees per second- and gradually increased to 0.5 degrees per second to generate a faster testing period while keeping data precise.

The failure modes of the pure tension and pure torsion tests matched expectations of brittle failure.

Brittle failure in tension experiences minimum plastic deformation so the surface is typically flat. The specimens' failure surface after the pure tension tests matched this expectation and was completely flat, as seen in Fig. B-1. In fact, if we were to attempt to piece the parts back together, the two would fit perfectly with very little material missing. If any material was missing, this could have been caused by a high testing rate that caused the material to violently rupture and get thrown from the specimen. Additionally, and differences in failure mode or stress values, such as the increased yield stress observed in test {1}, could also be attributed to increased strain or testing rate, or stress concentration conditions formed during the 3D printed process.

Brittle failure due to torsional loading occurs along planes perpendicular to the direction where tension is a maximum, typically along surfaces at 45° to the shaft's axis. The specimens' failure surface after the pure torsion tests matched this expectation and contained a 45° notch, as seen in Fig. B-2. All three specimens failed in the same direction; however, if any failed in the opposite direction, or didn't contain the 45° notch, this could be attributed to stress concentration conditions inadvertently formed during the 3D printed process.

Based on information available regarding brittle failure in tension and torsion, we expected that the failure mode of the combined loading tests to contain a mixture of both types of failure surfaces. The specimens' failure surface after the multiaxial tension-torsion test matched this expectation, containing both a flat failure surface and a 45° notch. However, while the blue specimen's notch matched those of the pure torsion test, the red and grey specimens had two notches surrounding an additional flat surface. The difference between these two types of multiaxial failure observed could be attributed to print quality of the specimens (the grey had several visible defects and cavities) or the testing rates used.

Based on the data collected during the tests that examined pure tensile failure behavior, the following yield and ultimate stress values were determined for the specimens used. It should be noted that since the material used (ABS plastic) is a brittle material, the yield stress and ultimate stress are the same.

Furthermore, when comparing the stress results to those in Table I and gathered previously by Cantrell et. al, the yield and ultimate strengths found in this experiment were significantly lower. Cantrell et. all tested ABS specimens in different orientations to determine mechanical properties; the yield stress and ultimate stress found for the "up-right" position specimens were 4,337 and 4,487 psi, respectively [11]. The difference in stress properties can likely be attributed to the print quality of the specimens, specifically the percent fill difference between Cantrell's standard dogbone specimens and the circular/hexagonal dogbone specimens used in the experiment.

TABLE II
Pure Tension - Yield and Ultimate Stress

Test {1}	2,498 psi
Test {2}	2,249 psi
Test {3}	2,237 psi
Average	2,328 psi

Similarly, based on the data collected during the tests that examined pure torsional failure behavior, the original data, and (12) and (13) were used to calculate the yield and ultimate stress values for the specimens used. In (12), T_Y is the torque value where yielding first occurs, C is the outside radius of the cross-section area of the circular test area only, and J is the polar moment of inertia of a hollow cylinder. In (13), D and d are the outer and inner diameters of the cross-section area of the circular test area, respectively.

$$\tau_Y = \frac{T_Y C}{J} \tag{10}$$

$$J = \frac{\pi(D^4 - d^4)}{32} \tag{11}$$

TABLE III
Pure Torsion - Yield and Ultimate Stress

Test {1} Yield	2,936 psi
Test {2} Yield	2,904 psi
Average Yield	2,920 psi
Test {1} Ultimate	3,394 psi
Test {2} Ultimate	3,406 psi
Average Ultimate	3,400 psi

Taking these average data values for pure tensile failure and pure torsional failure, we can accurately compare the failure criterion established by von Mises and Tresca in Fig. 2 to the failure criterion in Fig. 21.

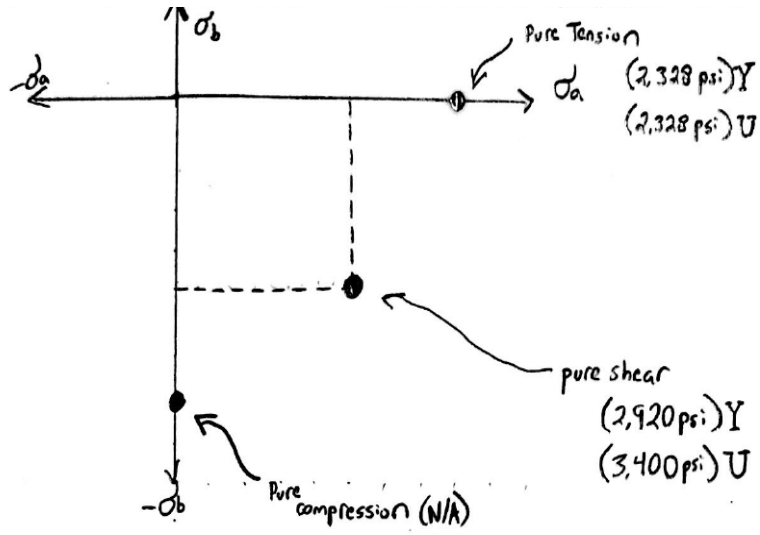

Fig. 21. Failure criterion based on average yield and ultimate data for the pure tension and pure torsion tests of the ABS specimens.

With the failure criterion established for pure tension and pure shear, we can begin to examine if the tests conducted accurately established where and when multiaxial failure would occur. To determine if the multiaxial tests accurately predicted or matched the failure criterion established in Fig. 21, the yield and ultimate stress values experience during the tension-torsion tests were found and complied into Table IV.

TABLE IV
Multiaxial Failure - Yield and Ultimate Stress

Test {1} Tension	Yield	1,664 psi
	Ultimate	1,695 psi
Test {1} Torsion	Yield	1,831 psi
	Ultimate	2,111 psi
Test {2} Tension	Yield	1,590 psi
	Ultimate	1,632 psi
Test {2} Torsion	Yield	1,923 psi
	Ultimate	2,094 psi
Test {3} Tension	Yield	1,462 psi
	Ultimate	1,488 psi

TABLE IV
Multiaxial Failure - Yield and Ultimate Stress

Test {3} Torsion	Yield	1,748 psi
	Ultimate	1,971 psi
Average Tension	Yield	1,572 psi
	Ultimate	1,605 psi
Average Torsion	Yield	1,834 psi
	Ultimate	2,059 psi

It should be noted that due to the combine loading, the yield and ultimate stress values were noticeably less than when the specimens were run under pure tension/torsion. The combined loading effects caused this dip due to the material being exposed to stress in every direction along its failure surface. Taking these average data values for multiaxial tensile/torsional failure, we can compare the pure tension/torsion failure criterion established in Fig. 21 to the combined failure criterion in Fig. 22.

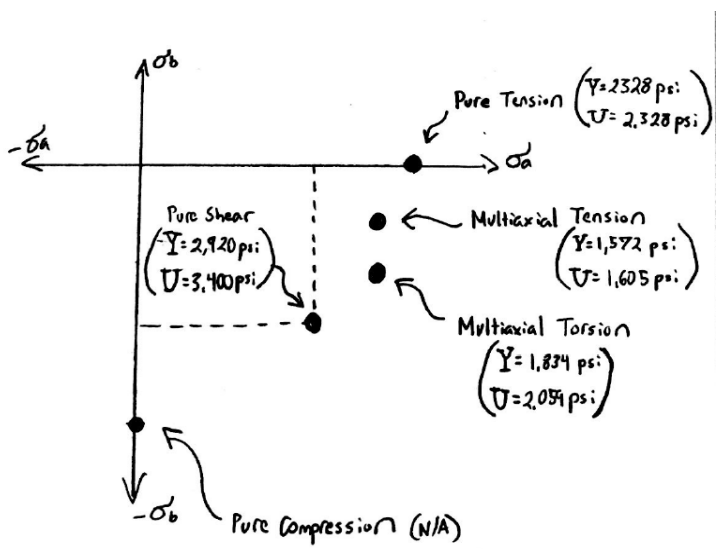

Fig. 22. Failure criterion based on average yield and ultimate data for the multiaxial tension/torsion tests of the ABS specimens, compared to failure criterion established from average yield and ultimate data for the pure tension and pure torsion tests.

SECTION V
CONCLUSION AND FUTURE WORK

In this thesis, we set out with the intent to develop testing methods that can be applied to the testing of brittle and ductile materials in one comprehensive failure test that will yield accurate failure criterion for combined tensile stress and torsional forces. To do this we studied the current failure criterion methods of a specific material (ABS plastic) to accurately describe and predict behavior of this material in between areas of pure shear and pure tension, i.e. multiaxial failure. ABS plastic was chosen as the testing material because of its predictable material properties and failure modes. To study the material, individual tensile and torsion tests were run to establish a baseline for the material's failure criterion. Then, multiaxial tests were run and compared to the established criterion. The behavior observed and the placement of the mixed tensile and torsional stress on the material's established failure graphs allowed us to see that the test method worked, and accurate results were achieved.

Despite the success of this experiment, several aspects need to be improved before other materials can be tested. One major problem encountered was misaligned chucks on the UTM; as the specimens were tightened into the grips, slight bending was observed which could have altered how or when the specimen failed. Another significant issue was poorly printed test specimens. Typical printing of the specimens took about 5-6 days; however, due to the timeframe of this experiment, some of the specimens had to be printed within 2-3 days. This rush could have caused significant cavities to form, resulting in stress concentrations that made the specimens fail faster than normal. Before testing can be carried to other materials, these two issues need to be corrected.

APPENDIX A
SOLIDWORKS MODEL DRAWINGS

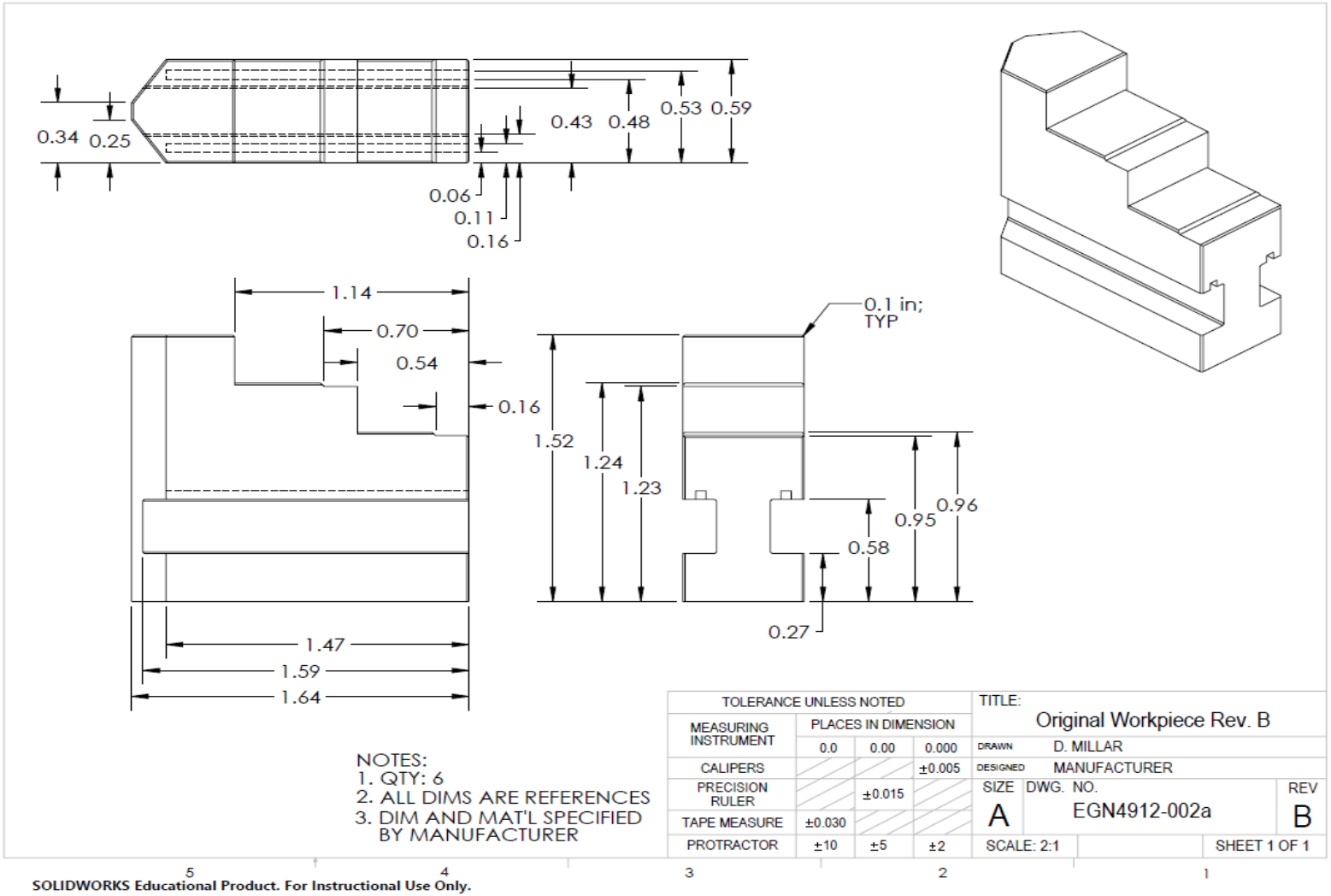

Figure A-1. Solidworks drawing of the original tension-torsion chuck grip.

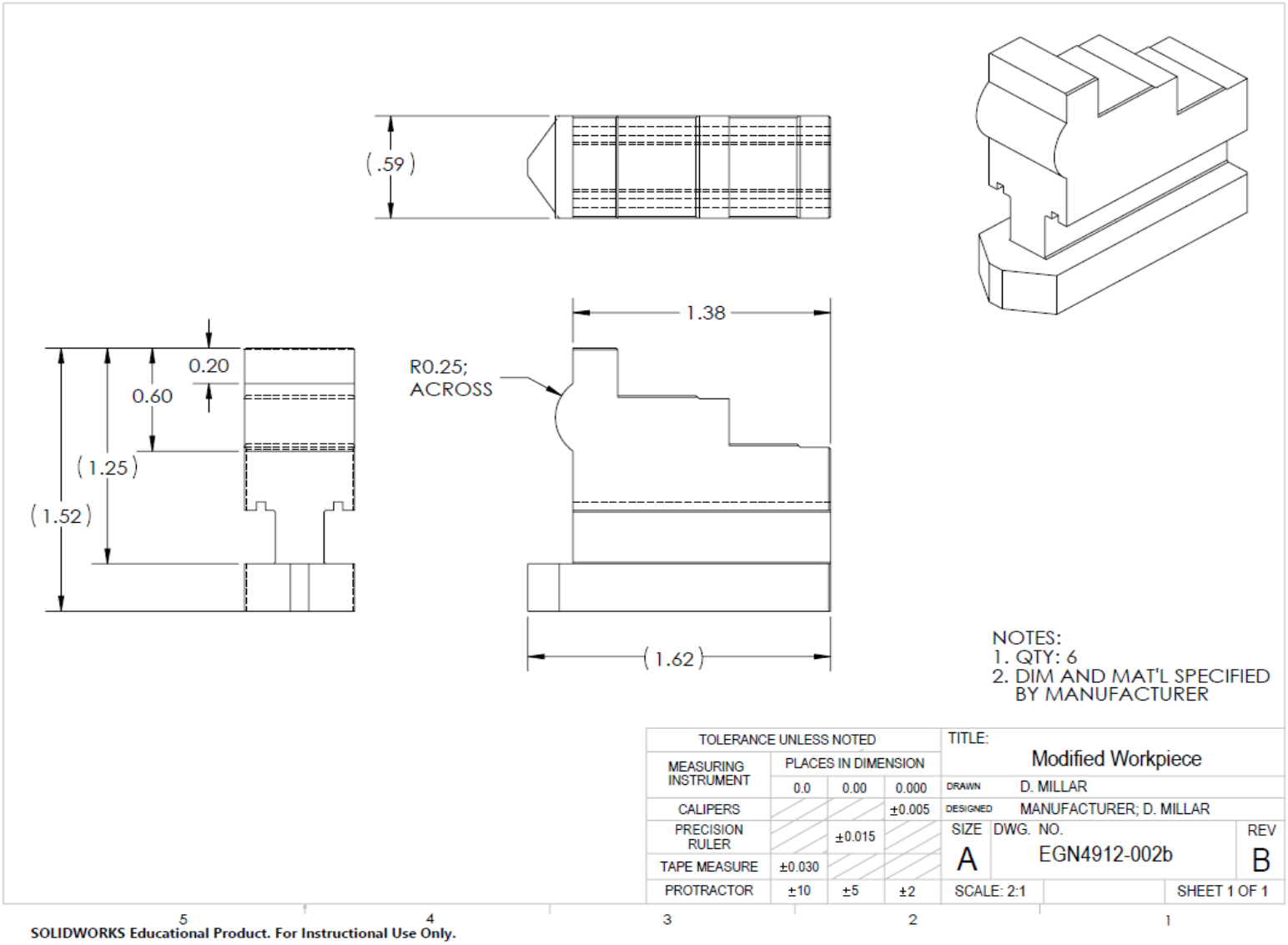

Figure A-2. Solidworks drawing of the desired modified tension-torsion chuck grip.

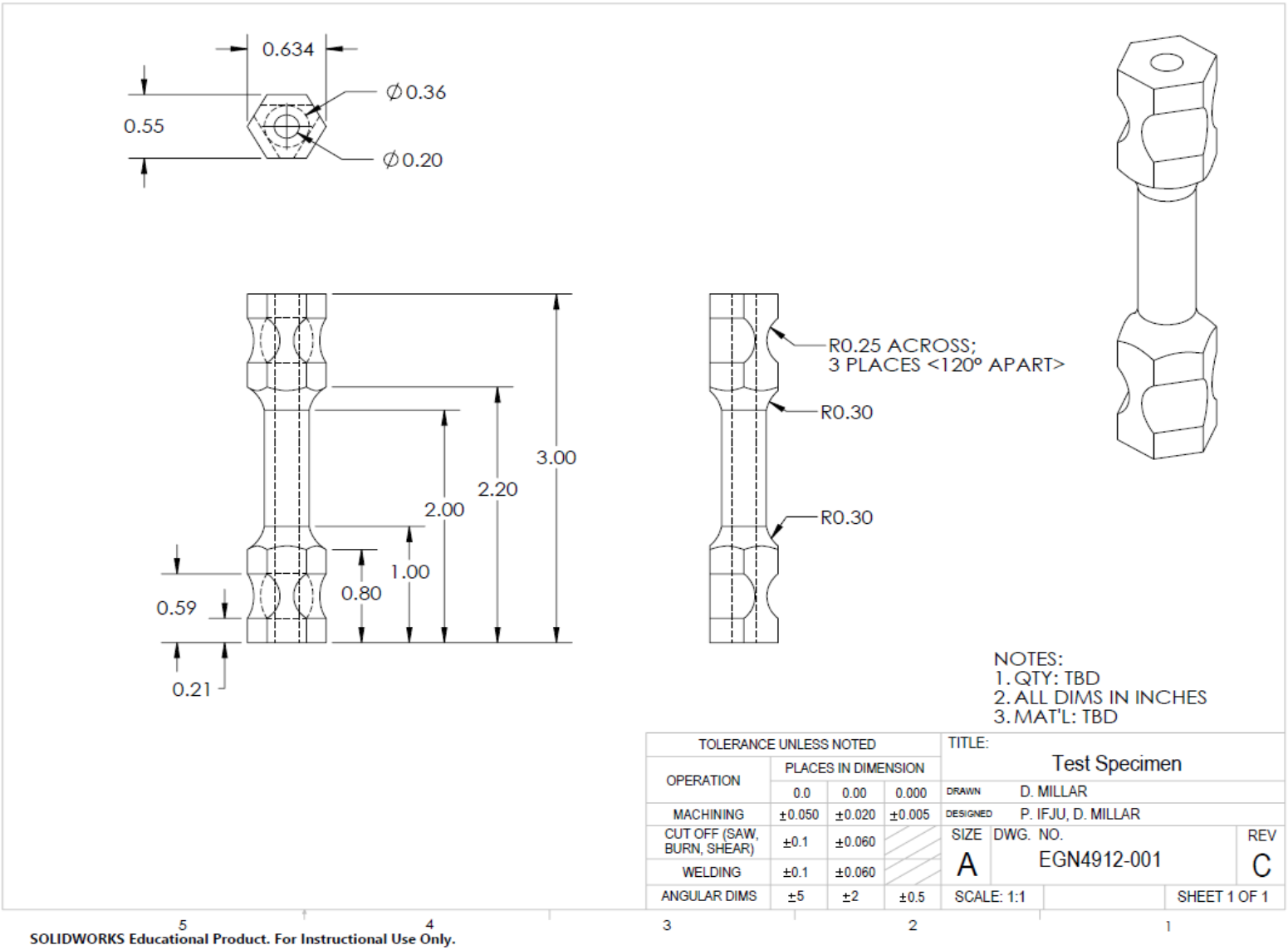

Figure A-3. Solidworks drawing of the hexagonal dogbone test specimen.

APPENDIX B
TEST SPECIMEN PICTURES

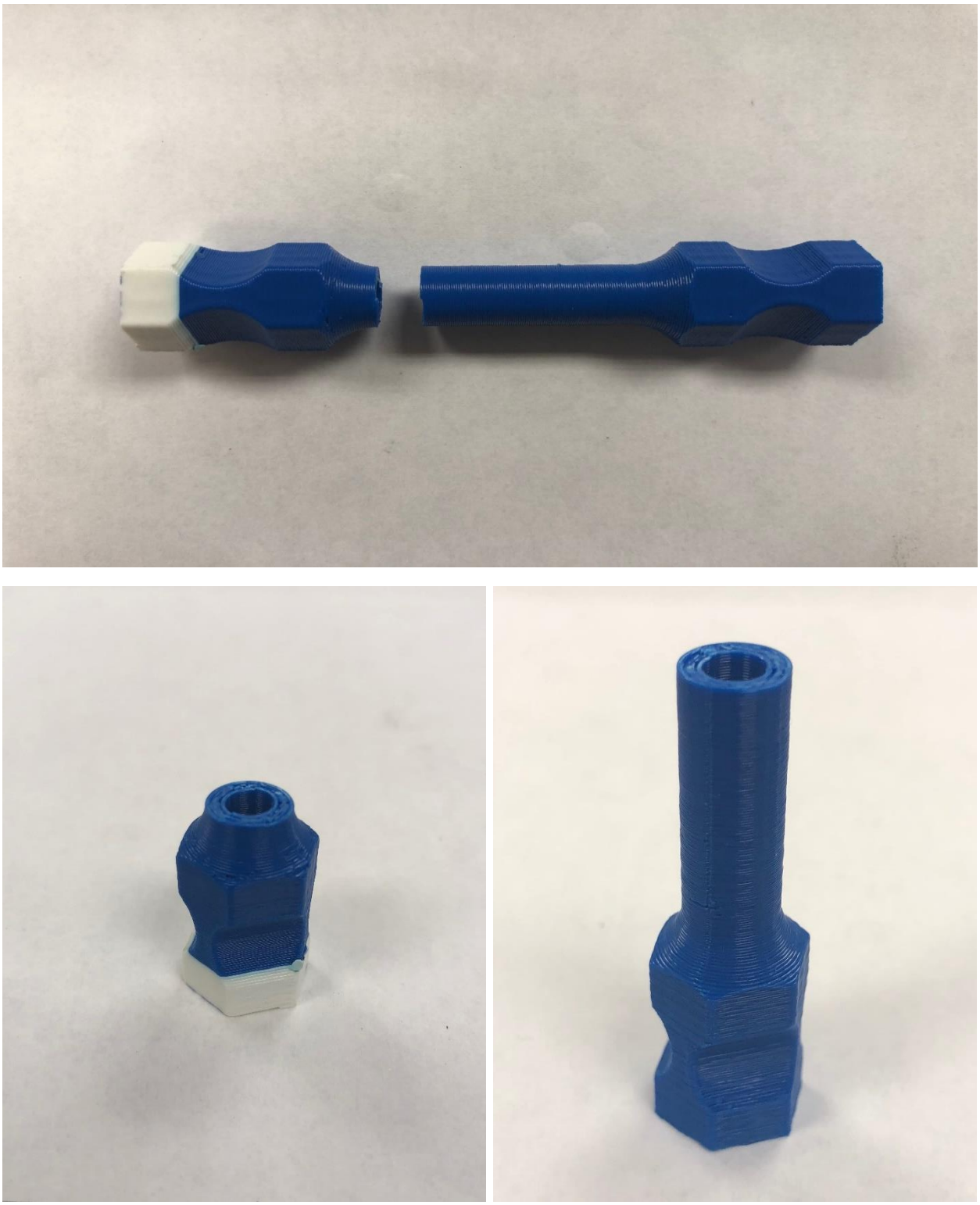

Fig. B-1(a)-(c). Dogbone specimen after failing during the pure tension test. The behavior exhibited is that of a brittle material due to the sudden rupture of the specimen without the presence of any plastic deformation, such as necking.

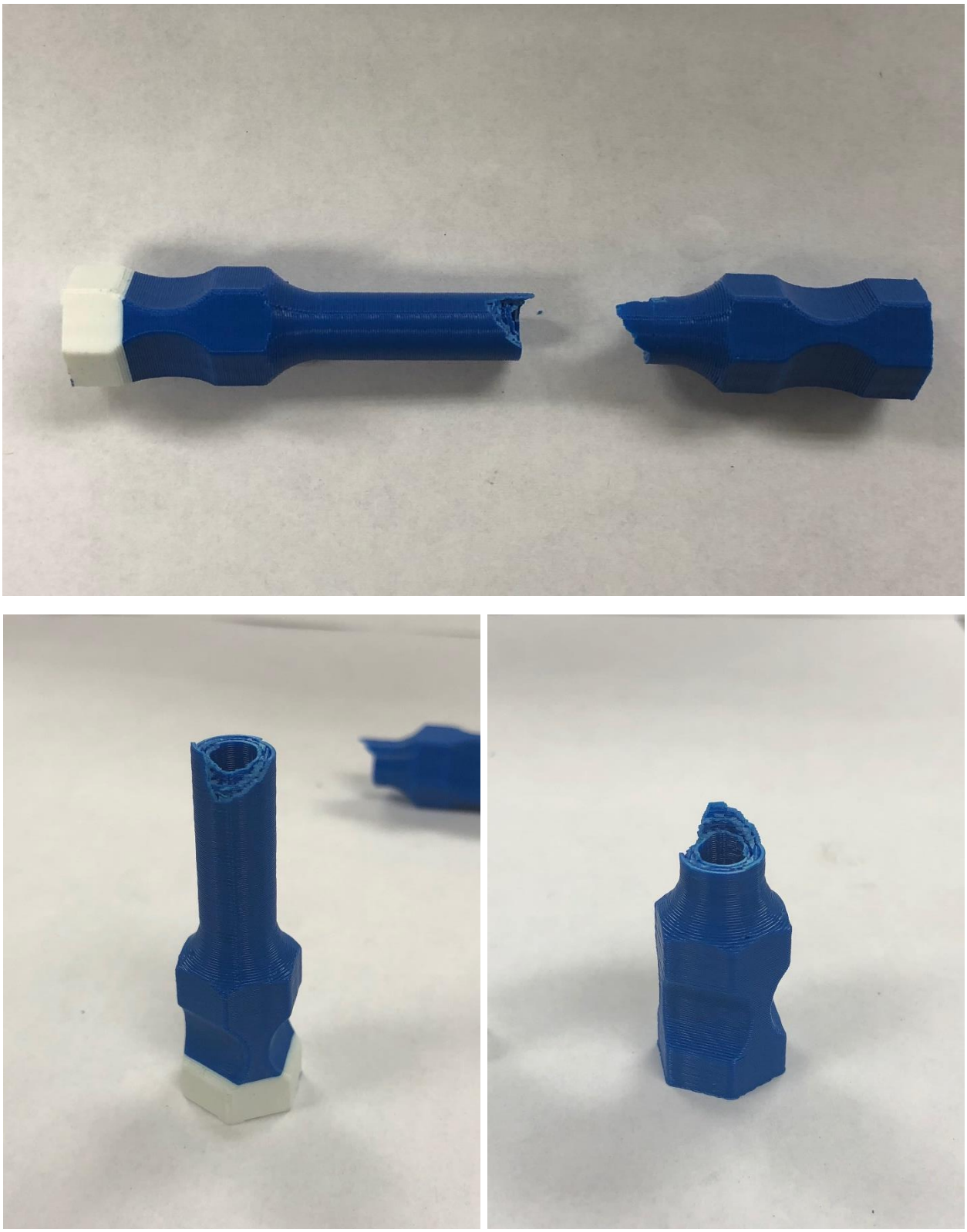

Fig. B-2(a)-(c). Dogbone specimen after failing during the pure torsion test. The behavior exhibited is that of a brittle material since the specimen failed along surfaces 45° to the shaft's axis.

Fig. B-3(a)-(c). Blue dog bone specimen after failing during the multiaxial tension-torsion test. The behavior exhibited is that of a brittle material and failed in tension (flat area) and torsion (45° to the shaft's axis).

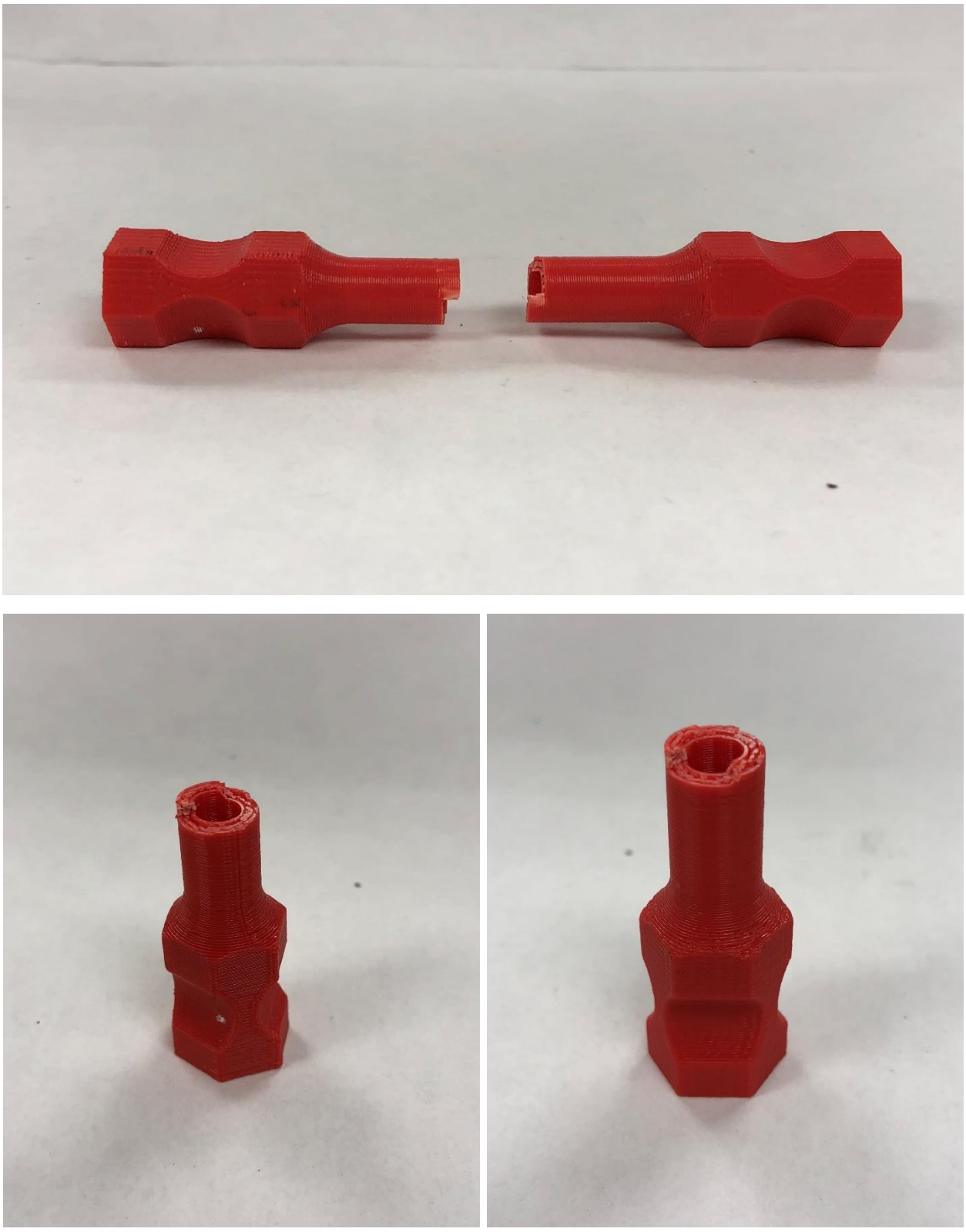

Fig. B-4(a)-(c). Red dog bone specimen after failing during the multiaxial tension-torsion test. The behavior exhibited is that of a brittle material and failed in tension (flat area) and torsion (45° to the shaft's axis).

LIST OF REFERENCES

[1] Filippini, M., Foletti, S. and Pasquero, G. (2010). Assessment of multiaxial fatigue life prediction methodologies for Inconel 718. *Procedia Engineering*, (2), pp.2347-2356.

[2] Nierenberger, M., Poncelet, M., Pattofatto, S., Hamouche, A., Raka, B. and Virely, J. (2011). Multiaxial Testing of Materials Using a Stewart Platform: Case Study of the Nooru-Mohamed Test. *Experimental Techniques*, (38), pp.74-83.

[3] Test Types. (2018). *Axial Torsion Test*. [online].

[4] Brannon, R. (2012). *Distinction between uniaxial stress and uniaxial strain*. [online].

[5] Kuhn, H. (1968). *Stress State in the Combined Stress Torsion Test*. Philadelphia: Drexel Institute of Technology Department of Metallurgical Engineering.

[6] Chandramouli, R. (n.d.). *Plasticity*. Thanjavur, India: SASTRA University.

[7] Beer, F., Johnston, Jr., E., DeWolf, J. and Mazurek, D. (2015). *Mechanics of Materials*. 7th ed. New York: McGraw Hill Education.

[8] Donohue, B. (2018). *How it Works – Wire EDM | Today's Machining World*. [online] Todaysmachiningworld.com.

[9] Xactedm.com. (2018). *What Is EDM? - How Does Electrical Discharge Machining Work?*: XACT. [online].

[10] Matweb.com. (2018). *MatWeb - The Online Materials Information Resource*. [online].

[11] Cantrell, J., Rohde, S., Damiani, D., Gurnani, R., DiSandro, L., Anton, J., Young, A., Jerez, A., Steinbach, D., Kroese, C. and Ifju, P. (n.d.). *Experimental Characterization of the Mechanical Properties of 3D-Printed ABS and Polycarbonate Parts*. Gainesville: UF Mechanical and Aerospace Engineering.

BIOGRAPHICAL SKETCH

Mr. David William Millar was born and raised up in Plantation, Florida, a suburb of Ft. Lauderdale, FL. He attended high school at South Plantation High School in Plantation and graduated in 2013. He continued his education at Broward College, graduate with his Associates of Arts degree in May 2015. After Broward College, David transferred to the University of Florida to pursue his Bachelor's degree in Mechanical Engineering. Meanwhile, he gained some research experience in the summer of 2017 by participating in the University of Michigan's Summer Research Opportunity Program. In the program, he worked under Dr. Bogdan Epureanu on a dissimilar materials project titled "Performance Prediction for Ultrasonic Spot-Welded Aluminum-Stainless Steel Specimens Exposed to Harmonic Loads and Material Degradation." In addition to his research, David also participated in a professional internship program at Walt Disney World. In this program, David worked at the Epcot Engineering Services department assisting current Imagineers with facilitating the design and installation of a maintenance bridge for the support team at the Frozen Ever After attraction, as well as enhancing ride components for the Test Track ride vehicles. David will be graduating magna cum laude from the University of Florida in May 2018 with his Bachelor's degree in Mechanical Engineering; he will then continue on at UF to pursue his Master's degree in Mechanical Engineering.